

# Adsorption of Proteins onto Surfaces Containing End-Attached Oligo(ethylene oxide): A Model System Using Self-Assembled Monolayers

Kevin L. Prime<sup>1</sup> and George M. Whitesides\*

Contribution from the Department of Chemistry, Harvard University, Cambridge, Massachusetts 02138

Received May 6, 1992. Revised Manuscript Received July 8, 1993\*

**Abstract:** This paper reports a study of the adsorption of four proteins—fibrinogen, lysozyme, pyruvate kinase, and RNase A—to self-assembled monolayers (SAMs) on gold. The SAMs examined were derived from thiols of the structure HS(CH<sub>2</sub>)<sub>10</sub>R, where R was CH<sub>3</sub>, CH<sub>2</sub>OH, and oligo(ethylene oxide). Monolayers that contained a sufficiently large mole fraction of alkanethiolate groups terminated in oligo(ethylene oxide) chains resisted the kinetically irreversible, nonspecific adsorption of all four proteins. Longer chains of oligo(ethylene oxide) were resistant at lower mole fractions in the monolayer. Resistance to the adsorption of proteins increased with the length of the oligo(ethylene oxide) chain: the smallest mole fraction of chains that prevented adsorption was proportional to  $n^{-0.4}$ , where  $n$  represents the number of ethylene oxide units per chain. Termination of the oligo(ethylene oxide) chains with a methoxy group instead of a hydroxyl group had little or no effect on the amount of protein adsorbed. The amount of pyruvate kinase that adsorbed to mixed SAMs containing hexa(ethylene oxide)-terminated chains depended upon the temperature. When the mole fraction of oligo(ethylene oxide) groups in the monolayer was below the level needed to prevent adsorption, more pyruvate kinase adsorbed to the monolayer at 37 °C than at 25 °C. No difference was observed between adsorption at 25 and 4 °C.

## Introduction

Materials presenting oligomers or polymers of ethylene oxide [–(CH<sub>2</sub>CH<sub>2</sub>O)<sub>*n*</sub>–, abbreviated as EO] on their surfaces are promising candidates for use in applications requiring contact with proteins, cells, and other biological systems.<sup>2–8</sup> We have prepared mono(mercaptoundecyl) ethers of a number of short oligomers of EO and used them to form self-assembled monolayers (SAMs) on gold. These SAMs present EO groups in controlled numbers at the solid–water interface.<sup>9</sup> Here we describe the influence of the length and number of EO chains upon the adsorption of proteins on these SAMs.

When hydrophobic colloids are treated with aqueous solutions containing poly(ethylene oxide) (PEO), the polymer adsorbs spontaneously at the colloid–solution interface.<sup>10,11</sup> Once the colloid surface has adsorbed significant amounts of PEO, it is stabilized against flocculation.<sup>10–13</sup> Similarly, block copolymers formed from PEO and a hydrophobic polymer adsorb to the surfaces of hydrophobic particles and stabilize the dispersion against flocculation.<sup>10</sup> The best stabilization to date—as measured

by surface force–balance techniques—has been achieved with chains that are tightly anchored at one end to the hydrophobic surface.<sup>12</sup> The anchoring “head group” must interact more strongly with the surface than does PEO. The needed selectivity has been achieved by physisorption<sup>13,14</sup> (as in the case of monoalkylated PEO surfactants, CH<sub>3</sub>(CH<sub>2</sub>)<sub>*x*</sub>(OCH<sub>2</sub>CH<sub>2</sub>)<sub>*y*</sub>OH), chemisorption<sup>15,16</sup> (e.g., amino-terminated PEO on mica), and covalent grafting.<sup>4,5</sup> The repulsive interactions between two surfaces bearing end-attached chains of PEO become significant at larger interparticle separations than those between two surfaces bearing randomly adsorbed PEO.<sup>12,13</sup>

Theoretical treatments of the stabilization of colloids by physio- and chemisorbed derivatives of PEO and other solvophilic polymers<sup>10,11</sup> are usually based on the concept of “steric repulsion”. These theories derive stabilization energies from one or both of two sources. First, as two polymer-coated colloidal particles collide, the polymer layers are compressed. The polymer chains have access to fewer configurations, and the resulting loss in entropy disfavors compression. Second, the collision expels solvent from the polymer surface layer. When the free energy of the solvent is lower in the solvent-swollen polymer layer than in the bulk, the energy required to desolvate the polymer layer disfavors compression of that layer. If these two stabilizing effects are energetic enough, the hydrophobic colloidal particles do not meet and do not flocculate.

The adsorption of proteins to polymer surfaces can be treated as a problem of colloidal stability in which the surfaces of the polymers and the proteins play the role of the hydrophobic colloids. Thus, it comes as no surprise that hydrophobic polymers to which PEO is either adsorbed or chemically grafted are resistant to the adsorption of proteins.<sup>17,18</sup>

Recently, Jeon and Andrade proposed a quantitative model for protein adsorption at a hydrophobic polymer surface to which

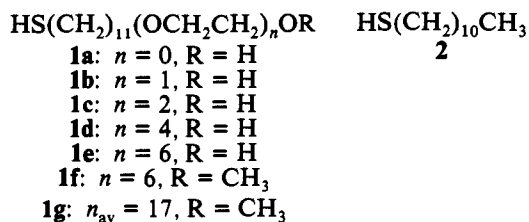
- \* Abstract published in *Advance ACS Abstracts*, September 1, 1993.  
 (1) Current address: Department of Chemistry, Mount Holyoke College, South Hadley, MA 01075.  
 (2) Merrill, E. W.; Salzman, E. W. *ASAIO J.* **1983**, *6* (2), 60–64.  
 (3) Gregonis, D. E.; Buerger, D. E.; Van Wagenen, R. A.; Hunter, S. K.; Andrade, J. D. *Trans. Soc. Biomaterials* **1984**, *7*, 766.  
 (4) Mori, Y.; Nagaoka, S.; Takiuchi, H.; Kikuchi, T.; Noguchi, N.; Tanazawa, H.; Noishiki, Y. *Trans. Am. Soc. Artif. Intern. Organs* **1982**, *28*, 459–463.  
 (5) Corrette, E.; Kishida, A.; Konishi, H.; Ikada, Y. *Polymers in Medicine III*; Migliaresi, C., Ed.; Elsevier: Amsterdam, 1988; pp 61–72.  
 (6) Grainger, D.; Okano, T.; Kim, S. W. *Advances in Biomedical Polymers*; Gebelein, C. G., Ed.; Plenum: New York, 1987; pp 229–247.  
 (7) Inada, Y.; Takahashi, K.; Yoshimoto, T.; Kodera, Y.; Matsushima, A.; Saito, Y. *TIBTECH* **1988**, *8*, 131–134.  
 (8) Kondo, A.; Kishimura, M.; Katoh, S.; Sada, E. *Biotech. Bioeng.* **1989**, *34*, 532–540.  
 (9) Pale-Grosdemange, C.; Simon, E. S.; Prime, K. L.; Whitesides, G. M. *J. Am. Chem. Soc.* **1991**, *113*, 12–20.  
 (10) Tadros, Th. F., Ed. *The Effect of Polymers on Dispersion Properties*; Academic: London, 1982.  
 (11) Sato, T.; Ruch, R. *Stabilization of Colloidal Dispersions by Polymer Adsorption*; Marcel Dekker: New York, 1980.  
 (12) Klein, J. *Phys. World* **1989**, *2*, 35–38.  
 (13) Klein, J. *Croat. Chem. Acta* **1990**, *63*, 441–454.

- (14) Claesson, P. M.; Kjellander, R.; Stenius, P.; Christenson, H. K. *J. Chem. Soc., Faraday Trans. 1* **1986**, *82*, 2735–2746.  
 (15) Claesson, P. M.; Gölander, C.-G. *J. Colloid Interface Sci.* **1987**, *117*, 366–373.  
 (16) Taunton, H. J.; Toprakcioglu, C.; Fetters, L. J.; Klein, J. *Nature* **1988**, *332*, 712–714.

PEO chains are terminally attached.<sup>19,20</sup> Their model pitted steric repulsion against both van der Waals attraction and the long-range hydrophobic attraction first reported by Pashley and co-workers.<sup>21,22</sup> (The long-range hydrophobic attraction decays exponentially with a characteristic length of 1.4 nm.) They calculated the free energies of adsorption of uniformly hydrophobic proteins—modeled as spheres of different radii—onto a planar hydrophobic surface bearing terminally attached PEO chains 80–120 residues long. The polymer chains were examined in the brush structure, where the average distance  $D$  between the chains was greater than the diameter of the chains in the crystal (0.463 nm) and less than the Flory radius  $R_F$  of the polymer.

Jeon and Andrade drew several conclusions: (i) that a weak, long-range hydrophobic attraction between PEO and protein competes with repulsion and determines the resistance of the surface to the adsorption of protein, (ii) that the concentration of PEO chains in the interface required to resist the adsorption of protein decreases as the size of the protein increases, and (iii) that surfaces comprising densely packed, nearly crystalline chains of PEO might not resist the adsorption of protein.

Despite the growing body of theoretical and experimental work on these materials, the length and number of EO chains at the solid–solution interface that are required for resistance to protein adsorption have remained poorly defined. We sought a convenient experimental means to test the effects of grafting density and polymer length upon the resistance properties of the surface. Recently, we reported that SAMs containing appropriate concentrations of hexa(ethylene oxide)-terminated chains [S-(CH<sub>2</sub>)<sub>11</sub>(OCH<sub>2</sub>CH<sub>2</sub>)<sub>6</sub>OH, abbreviated as SC<sub>11</sub>E<sub>6</sub>OH, **1e**] resist the adsorption of proteins.<sup>23</sup> Figure 1 is a schematic illustration of a SAM comprising a mixture of S(CH<sub>2</sub>)<sub>10</sub>CH<sub>3</sub> (abbreviated as SC<sub>10</sub>CH<sub>3</sub>) and SC<sub>11</sub>E<sub>6</sub>OH. Water is a good solvent for PEO, and in contact with water, the EO chains in the SAM are self-avoiding and tend to form *gauche* bonds.<sup>24</sup> The monolayer–solution interface of these SAMs corresponds to the interfacial structures of hydrophobic polymers bearing end-grafted PEO chains.



SAMs make particularly good model systems for the study of protein–surface interactions. They are easily prepared.<sup>25</sup> Their topology is controlled by the topology of the underlying gold substrate, which is nearly constant from sample to sample. SAMs of  $\omega$ -substituted alkanethiols [S(CH<sub>2</sub>) <sub>$n$</sub> R,  $n \geq 10$ , R = a functional group with a cross section no larger than that of a CH<sub>2</sub> group] comprise densely packed, pseudocrystalline arrays of predominantly *trans*-extended chains oriented with their sulfur termini at the gold–SAM interface.<sup>26</sup> Thus, the properties of the SAM–solution interface can be controlled by varying R during

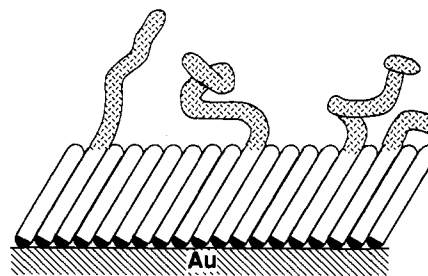
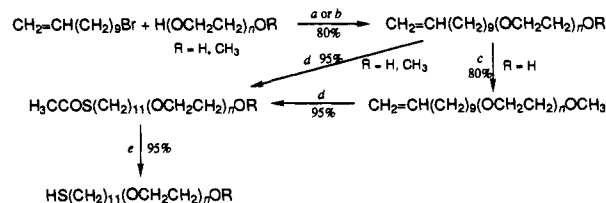


**Figure 1.** Schematic representation of the structure of a mixed SAM containing SC<sub>11</sub>E<sub>6</sub>OH and SC<sub>10</sub>CH<sub>3</sub>. The oligo(ethylene oxide) chains are flexible. The areas of the hatched regions are approximately proportional to the cross sectional area of the E<sub>6</sub>OH chain.

### Scheme I. General Synthesis of Derivatives of Oligo(ethylene oxides), HSC<sub>11</sub>E <sub>$n$</sub> OR<sup>a</sup>



<sup>a</sup> (a) Aqueous NaOH, 100 °C; (b) NaH, DMF; (c) KOH, CH<sub>3</sub>I, DMSO; (d) CH<sub>3</sub>COSH, AIBN, THF and (e) HCl, MeOH.

the synthesis of the precursor alkanethiols.<sup>27</sup> Further control over the interfacial properties of the SAM is possible through the preparation of “mixed” SAMs by adsorption from solutions containing mixtures of alkanethiols.<sup>28–30</sup> SAMs, therefore, allow the study of protein–surface interactions with well-defined substrates capable of presenting a wide variety of functional groups alone and in combination at the surface–solution interface.

We have examined the effects of the length and number of ethylene oxide (E <sub>$n$</sub> ) chains upon the protein resistance of SAMs. Even short (E<sub>1</sub>) ethylene oxide chains prevented protein adsorption when they accounted for almost all of the chains in the SAM. Terminally attached PEO oligomers ( $n \geq 2$ ) prevented adsorption when present in numbers greater than a threshold value, even in the limit of a densely packed monolayer. The threshold of resistance to protein adsorption was dependent upon the length of the EO chains. The detailed adsorption profile of pyruvate kinase was dependent upon the temperature at which the adsorption experiment was performed.

## Results

**Synthesis of Thiols.** Thiols **1a**, **1d**, **1e**, and **2** were available from previous studies.<sup>9</sup> Thiols **1b**, **1c**, **1f**, and **1g** were prepared according to Scheme I. Details are provided in the supplementary material.

Monodisperse E <sub>$n$</sub>  precursors were not commercially available for  $n \geq 6$ . The longest compound (**1g**) was prepared from a polymer (HE <sub>$n$</sub> OCH<sub>3</sub>). The average molecular weight of the precursor was 750, corresponding approximately to E<sub>17</sub>. We use brackets to signify the average chain length of a polydisperse oligomer, *e.g.*, (**17**), and thus SC<sub>11</sub>E<sub>(17)</sub>OCH<sub>3</sub> represents a mixture of compounds with an average of 17 ethylene oxide units per chain.

**Preparation and Characterization of SAMs.** Polycrystalline gold films (200-nm thick) were deposited by evaporation of gold

(26) Nuzzo, R. G.; Dubois, L. H.; Allara, D. L. *J. Am. Chem. Soc.* **1990**, *112*, 558–569.

(27) Bain, C. D.; Evall, J.; Whitesides, G. M.; Nuzzo, R. G. *J. Am. Chem. Soc.* **1989**, *111*, 7155–7164.

(28) Bain, C. D.; Whitesides, G. M. *J. Am. Chem. Soc.* **1988**, *110*, 6560–6561.

(29) Bain, C. D.; Whitesides, G. M. *Science* **1988**, *240*, 62–63.

(30) Bain, C. D.; Whitesides, G. M. *J. Am. Chem. Soc.* **1988**, *110*, 3665–3666.

(17) Stenius, P.; Berg, J.; Claesson, P.; Gölander, C. G.; Herder, C.; Kronberg, B. *Croat. Chem. Acta* **1990**, *63*, 501–516. Gölander, C. G.; Kiss, E. *J. Colloid Interface Sci.* **1988**, *121*, 240–53. See also refs 1–3, 5, and 8.

(18) While PEO-derived materials are an excellent choice for applications requiring *in vitro* compatibility with proteins, their ultimate utility as long-term biocompatible materials remains unclear (ref 5).

(19) Jeon, S. I.; Lee, J. H.; Andrade, J. D.; De Gennes, P. G. *J. Colloid Interface Sci.* **1991**, *142*, 149–158.

(20) Jeon, S. I.; Andrade, J. D. *J. Colloid Interface Sci.* **1991**, *142*, 159–166.

(21) Israelachvili, J. N.; Pashley, R. M. *J. Colloid Interface Sci.* **1984**, *98*, 500–514.

(22) Pashley, R. M.; McGuiggan, P. M.; Ninham, B. W. *Science* **1985**, *229*, 1088–1089.

(23) Prime, K. L.; Whitesides, G. M. *Science* **1991**, *252*, 1164–1167.

(24) Matsuura, H.; Fukuhara, K. *J. Mol. Struct.* **1985**, *126*, 251–260.

(25) Whitesides, G. M.; Laibinis, P. E. *Langmuir* **1990**, *6*, 87–96.

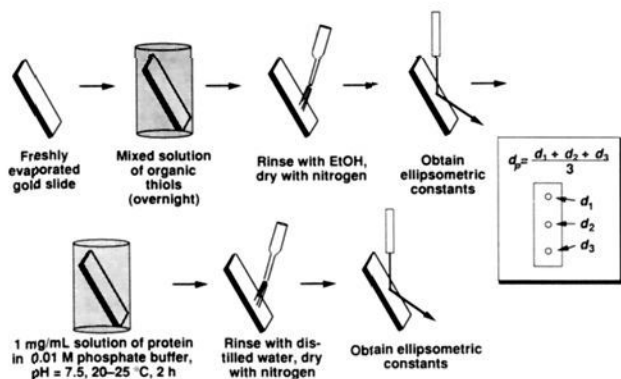


**Figure 2.** Schematic representation of the protocol used to determine the amount of adsorbed protein on each SAM. First, each SAM was formed on a freshly evaporated Au substrate, washed with ethanol, and dried with a stream of  $N_2$ . Ellipsometric constants were obtained from three locations on the SAM. It was then immersed in a solution of protein in aqueous phosphate buffer for 2 h, rinsed with distilled water, and dried with a stream of  $N_2$ . A second set of ellipsometric constants was obtained, and the nominal thickness of the adsorbed film of protein  $d_p$  was calculated for each of the three locations on the slide. Those values were averaged to obtain the values plotted in the following figures.

onto chromium-primed silicon wafers.<sup>31</sup> These films were immersed for 12 h to 1 week in ethanol solutions containing mixtures of **1** and **2** in different relative concentrations. The total concentration of thiol in each solution was 0.25 mM.<sup>32</sup> Each SAM was characterized by X-ray photoelectron spectroscopy (XPS) and by measurement of its maximum advancing and minimum receding contact angles with water<sup>33</sup> ( $\theta_a(H_2O)$  and  $\theta_r(H_2O)$ , respectively). The average thicknesses of mixed SAMs formed from **1g** and **2** were measured by ellipsometry.

Since **2** was one of the two components in every mixed SAM described here, we shall use the shorthand phrase "mixed SAM of X" to refer to a SAM prepared from a solution that contained a mixture of X and **2**. For the sake of clarity, we shall also use the phrase "pure SAM of X" to refer to a SAM prepared from a solution that contained only X.

The mole fraction of **1** ( $\chi_1$ ) in each mixed SAM of **1a-f** was calculated by comparing the area under the O(1s) photoelectron peak of the mixed SAM ( $I_{1,2}^{O(1s)}$ ) with the area under the O(1s) peak of a pure SAM of **1** ( $I_1^{O(1s)}$ ):  $\chi_1 = I_{1,2}^{O(1s)} / I_1^{O(1s)}$ .<sup>34</sup> Due to attenuation of the photoelectrons by the SAMs, the O(1s) signal from mixed SAMs of **1g** was not a linear function of the thickness of the SAM as measured by ellipsometry. Therefore, we determined the values of  $\chi_1$  for mixed SAMs of **1g** by comparing their ellipsometric thicknesses to those of pure SAMs of **1g** and of **2**. We estimate that the values of  $\chi_1$  derived from XPS and ellipsometry data are accurate to  $\pm 0.05$ .

**Protein Adsorption.** Figure 2 is a schematic representation of the protocol we used for forming the SAMs and measuring the amounts of proteins that adsorbed to them.<sup>35</sup> The SAMs were removed from the solutions in which they were prepared, rinsed

thoroughly with ethanol, and dried with a stream of nitrogen. They were then immersed for 2 h in solutions containing 1 mg/mL of protein in 10 mM aqueous sodium phosphate buffer at pH 7.5 and 20–25 °C.<sup>34</sup> The amount of protein that remained on each SAM after it had been rinsed with water was determined by ellipsometry. Three measurements of  $d_p$  were made at different positions on each SAM; the value reported for each SAM is the average of these three measurements.

The calculation of  $d_p$  from the experimentally obtained ellipsometric constants required that those constants be interpreted in light of some model of the interface. We applied a standard, homogeneous three-layer (substrate–film–ambient) model.<sup>36</sup> This model contains three unknowns: the thickness ( $d_p$ ), refractive index ( $n_p$ ), and extinction coefficient ( $k_p$ ) of the adsorbed protein film. (The refractive index and the extinction coefficient are the real and complex parts, respectively, of the complex refractive index  $N_p = n_p + k_p i$ .) Either  $n_p$  or  $d_p$ , but not both, can be determined analytically from the specific type of experiment we employed.<sup>37</sup> We assumed values of  $n_p = 1.45$  and  $k_p = 0$  for all the proteins. This approach offered an uncomplicated, rapid method for determining the *relative* amounts of proteins adsorbed on the surface without prior knowledge of the optical properties of the film of protein (which are frequently unknown).

Our model assumes that incomplete films of proteins are continuous layers with thicknesses  $d_p = \rho d_{max}$ , where  $\rho$  is the fractional coverage of the surface and  $d_{max}$  is the thickness observed for pure SAMs of **2**. Real protein films are likely to have structures more closely resembling islands with thickness  $d_{max}$  covering a fraction  $\rho$  of the surface. By assuming a constant thickness for the protein molecule, calculating values of  $n_p$  from the ellipsometric data, and applying the approach of Maxwell Garnett,<sup>38</sup> one can calculate the value of  $\rho$  for an island model. With our samples, the difference between the values of  $\rho$  obtained by the continuous and island models was always equal to or smaller than the scatter in our data. Because the two models gave experimentally indistinguishable results, we continued to employ the more convenient continuous model.

The assumption of a common value for  $n_p$  leads to two qualifications to the values of  $d_p$  reported here: First, the values of  $d_p$  for different proteins may not be directly comparable, since the values of  $n_p$  for these proteins may differ slightly. The values of  $n_p$  for proteins adsorbed at interfaces usually fall between 1.35 and 1.55.<sup>39</sup> When we calculated values of  $d_p$  using  $n_p = 1.33$ , the values of  $d_p$  were 25% higher than the values of  $d_p$  calculated using  $n_p = 1.45$ . A 25% decrease in the values of  $d_p$  relative to those obtained for  $n_p = 1.45$  required  $n_p = 1.71$ . We conclude that the true values of  $d_p$  differ from the values we have calculated by no more than  $\pm 25\%$ . Second, if  $n_p$  varies with the amount of a given protein that is adsorbed, the shapes of the curves in Figures 3 and 5 will be distorted. Changes in the value of  $n_p$  could occur were the protein to undergo conformational changes upon adsorption, thereby changing the ratio of protein to water in the film. As we noted above, the value of  $d_p$  is relatively insensitive to changes of  $\pm 0.05$  in  $n_p$ ; changes in the balance of protein and water in the adsorbed film should cause only small changes in the value of  $n_p$ . We conclude that it is unlikely that errors arising from variation in  $n_p$  with the amount of adsorbed protein have any significant effect upon the shapes of the curves in Figures 3

(31) Gold films prepared in this manner are polycrystalline. However, the crystal faces are sufficiently large that the SAMs consist primarily of molecules in planar assemblies. Considerably less rough gold can be prepared by more elaborate methods than those applied here, but the resulting SAMs have wetting properties almost indistinguishable from those of the SAMs reported in this paper. We therefore think that the use of flat gold films would lead to the same conclusions and almost indistinguishable experimental results as those reported here.

(32) At this concentration, complete monolayers form in much less than 12 h. Although the compositions of some mixed SAMs have been shown to vary with the time of immersion (Folkers, J. P.; Whitesides, G. M. Personal communication), we observed no such change in the compositions of mixed SAMs of  $SC_{11}E_{18}OR$  over a period of several weeks. We therefore prepared gold substrates in large batches, immersed the slides in the adsorption solutions within an hour, and removed the slides as they were needed for further experiments.

(33) Dettre, R. H.; Johnson, R. E. *J. Phys. Chem.* **1965**, *69*, 1507–1515.

(34) A detailed analysis of this method is provided in the supplementary material.

(35) This procedure is the same as that used in ref 23 with the exception that the time of immersion is 2 h rather than 1 h. We have found that the amount of adsorbed protein does not change significantly after 2 h for the four proteins we studied.

(36) McCrackin, F. L.; Passaglia, E.; Strömberg, R. R.; Steinberg, H. L. *J. Res. Natl. Bur. Stand., Sect. A* **1963**, *67*, 363–377.

(37) Azzam, R. M. A.; Bashara, N. M. *Ellipsometry and Polarized Light*; North-Holland: Amsterdam, 1987.

(38) Maxwell Garnett, J. C. *Phil. Trans.* **1904**, *203*, 385. Maxwell Garnett, J. C. *Phil. Trans.* **1906**, *205*, 237.

(39) Arnebrant, T.; Ivarsson, B.; Larsson, K.; Lundström, I.; Nylander, T. *Prog. Colloid Polym. Sci.* **1985**, *70*, 62–66. Cuyper, P. A.; Hermens, W. T.; Hemker, H. C. *Anal. Biochem.* **1978**, *84*, 56–67.

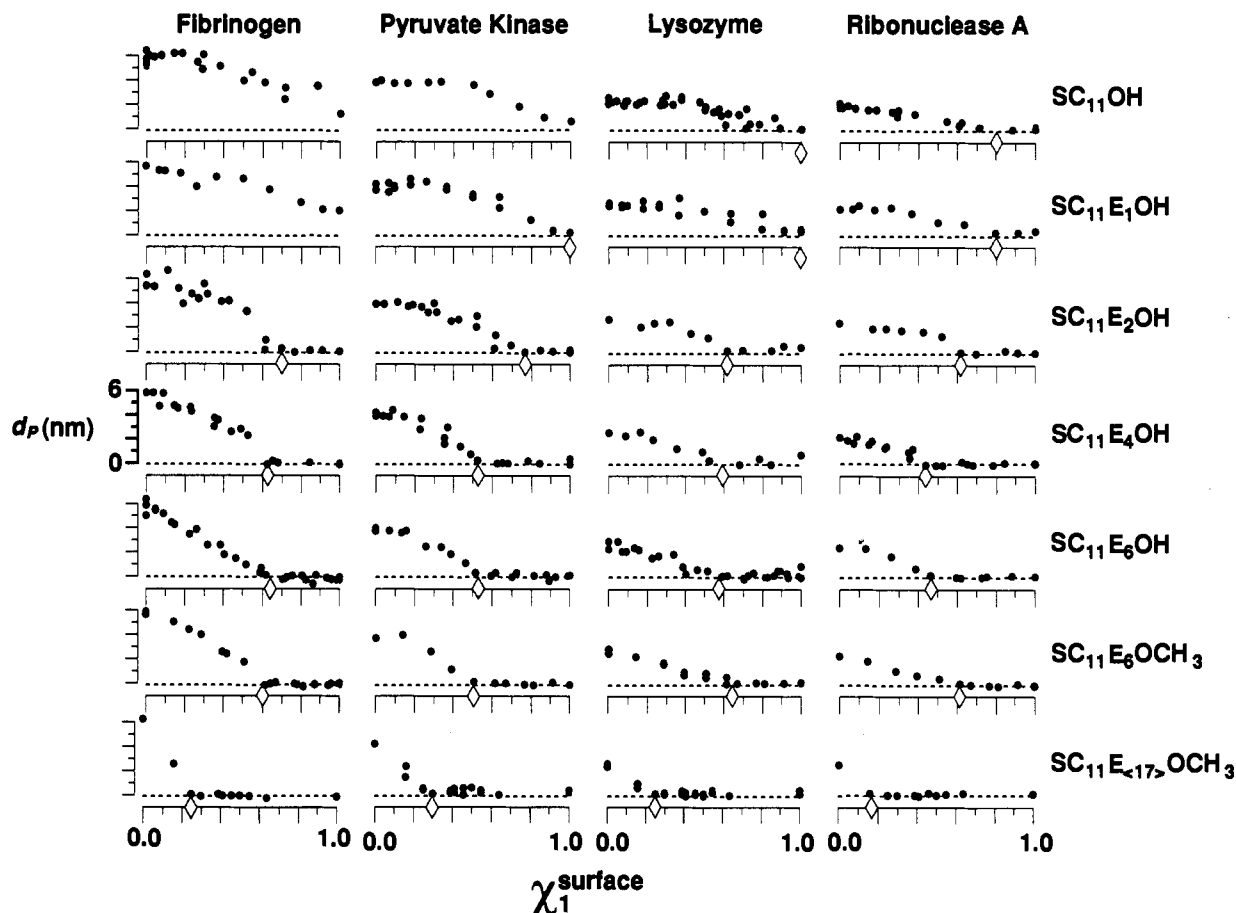


**Figure 3.** Nominal thickness ( $d_p$ ) as a function of  $\chi_1$ . Adsorption of fibrinogen, pyruvate kinase, lysozyme, and ribonuclease A to mixed SAMs of  $SC_{11}E_nOR$  decreases as the number or the length of the  $SC_{11}E_nOR$  chains increases. The nominal thickness  $d_p$  of the adsorbed films of the four proteins on mixed SAMs containing  $SC_{11}E_nOR$  is plotted as a function of  $\chi_1$ , the mole fraction of  $SC_{11}E_nOR$  chains in the SAM. The values of  $d_p$  were determined by ellipsometry and represent the average of three measurements made at different positions on a single sample. The values of  $\chi_1$  were determined prior to the adsorption of protein. For  $SC_{11}E_nOR$  ( $n \leq 6$ ), the values of  $\chi_1$  are the normalized intensities of the O(1s) photoelectron signals from the SAMs; for  $SC_{11}E_{(17)}OCH_3$ , they are the normalized thicknesses of the SAMs, as determined by ellipsometry. The diamonds on the horizontal axes denote estimated values of  $\chi_1^{resist}$ . The horizontal and vertical scales are uniform throughout the figure.

and 5. Supporting evidence for these two conclusions is presented in the supplementary material.

The ellipsometric protocol we employed required that the protein films be dried with a stream of nitrogen before being analyzed. This step was required to prevent any physisorbed water from contributing to the value of  $d_p$ . We do not know the extent to which the drying step perturbed the structures of the proteins.<sup>40</sup> Therefore, the values of  $d_p$  are best interpreted as measures of the relative amounts of protein adsorbed to the SAMs, not as measures of the absolute thicknesses of these protein films when in contact with solutions containing proteins.

**Stability of the SAMs.** We subjected pure SAMs of each of the alkanethiols used in this study to the protein adsorption protocol summarized in Figure 2, omitting the protein from the buffer solution. The ellipsometric thicknesses, XPS spectra, and contact angles of the SAMs were unchanged by this treatment. This result demonstrates that the SAMs remained intact under the conditions of the experiment.

**Relationship between Protein Adsorption and Composition of the SAM.** Figure 3 shows the nominal thickness of the adsorbed film ( $d_p$ ) of four proteins on seven series of mixed SAMs of **1** as a function of  $\chi_1$ . In order to facilitate discussion of the data, we

(40) Nor do we know the extent to which water in the solvated PEO film is trapped in the film by adsorption of protein. This water, which was not present during the preliminary ellipsometric measurement, would increase the apparent thickness of the film. The data in this paper lead to the conclusion that proteins do not adsorb to those parts of the SAM that are predominantly composed of hydrated PEO chains. Thus, we think that the PEO chains are as exposed to the drying process as those in the bare monolayer and that the contribution of trapped water to the value of  $d_p$  is minimal.

define  $\chi_1^{resist}$  as the minimum value of  $\chi_1$  for which  $d_p = 0$ . We highlight several significant observations from these data.

**1. SAMs that Contained Appropriately High Concentrations of  $E_n$  Chains Resisted the Adsorption of Proteins.** This resistance was the most significant feature of the mixed SAMs of **1**. We could not detect the presence of protein on these surfaces by ellipsometry, XPS [N(1s)], or contact angle measurement.

Some caution in interpreting these results is warranted. We use  $d_p = 0$  as the operational definition of resistance to protein adsorption. Whether resistance is observed for any given SAM is therefore dependent upon our protocol for measuring  $d_p$ . A value of  $d_p = 0$  should not be interpreted to mean that no protein adsorbed to the SAM *in situ* but only that any adsorbed protein was easily removed by gentle rinsing. *Indeed, all of the SAMs emerged from the protein solutions completely wet by the solution. SAMs for which  $d_p = 0$  regained their receding contact angles with water—characteristic of SAMs containing high mole fractions of **1**—only after the first rinse.* We will consider this observation more thoroughly in the Discussion.

**2. Longer  $E_n$  Chains Resisted Adsorption More Effectively Than Shorter Chains.** This trend was manifested in two ways: First, the value of  $\chi_1^{resist}$  decreased between  $n = 1$  and  $n = (17)$ . Second, the slope of the curve derived from the data at low values of  $\chi_1$  became more negative as  $n$  increased.

**3. A Terminal Hydroxyl Group Was Not Required To Prevent Adsorption of Proteins.** Mixed SAMs of  $SC_{11}E_6OCH_3$  resisted adsorption of proteins almost as well as mixed SAMs of  $SC_{11}E_6-$

OH; the introduction of a methyl ether had essentially no effect upon the ability of the SAMs to resist the adsorption of proteins.

**4. The Results Were Reproducible.** The data shown in Figure 3 represent one to three experiments for each curve. Whenever more than one independent experiment was performed, the curves were superimposable within experimental error. The scatter in the ellipsometric thicknesses of adsorbed protein films—as determined from three different locations on the sample—was sometimes two to three times greater than the corresponding scatter in the thicknesses of SAMs of *n*-alkanethiols, particularly at values of  $\chi_1$  for which  $d_p$  was changing most rapidly. Occasionally, this scatter was sufficient to cause the data to fall well away from the curves represented here. We have removed outliers from the figures presented here to improve clarity; in no case do they represent more than 1 in 20 of the measurements made.

**Relationship between Wettability and Composition of the SAM.**

Figure 4 shows the maximum advancing and minimum receding contact angles of water on the SAM as a function of  $\chi_1$ . Above a certain value of  $\chi_1$ —different for each compound **1a–g**—mixed SAMs of **1** were as wettable as pure SAMs of **1**. This observation implies that these mixed SAMs of **1** presented an interface that consisted almost entirely of  $E_n$  groups. Not surprisingly, then, the values of  $\chi_1^{\text{resist}}$  for each protein occurred near the lowest value of  $\chi_1$  at which the wettability of the mixed SAM of **1** was indistinguishable from that of a pure SAM of **1**.

Others have proposed a number of methods for relating the solid–water interfacial energy of a material to its protein resistance or biocompatibility.<sup>41</sup> Real materials sometimes show large differences between  $\theta_a(\text{H}_2\text{O})$  and  $\theta_r(\text{H}_2\text{O})$ ; it is not clear whether either measurement should provide a predictor of resistance to protein adsorption. Figure 4 shows that mixed SAMs of **1** on gold that resisted protein adsorption also exhibited low and nearly constant hysteresis. In the following section, we plot  $d_p$  as a function of  $\cos \theta_a(\text{H}_2\text{O})$ ; examination of the data using  $\cos \theta_r(\text{H}_2\text{O})$  yielded no new information.

**Relationship of Protein Adsorption to Wettability of the SAMs.**

Figure 5 shows the thickness,  $d_p$ , of the adsorbed films of fibrinogen, pyruvate kinase, lysozyme, and ribonuclease A as a function of  $\cos \theta_a(\text{H}_2\text{O})$  for the SAMs that we examined. These figures present a number of important observations.

**1. Protein Adsorption Was Frequently More Sensitive Than Wettability to the Presence of the Hydrophobic Component of the Mixed SAMs.** This sensitivity was reflected in the upward curvature of many of the plots in Figure 5. For the most hydrophilic surfaces, small changes in the wettability of the surface often produced large changes in the amount of protein adsorbed. In a number of instances, significant increases in protein adsorption occurred before any change in the wettability of the SAMs could be detected.

**2. For a Given Hydrophilic Component, Resistance to Protein Adsorption Increased with the Hydrophilicity of the Interface.** The amount of adsorbed protein decreased monotonically—although not linearly—in all cases. This observation is consistent with a large body of experimental data<sup>42</sup> but does not establish whether the dominant variable is the concentration of the hydrophilic component in the interface or the wettability of the interface.

**3. Homologous Hydrophilic Groups Had Similar Properties of Resistance to Protein Adsorption.** The curves obtained by plotting  $d_p$  as a function of  $\cos \theta_a(\text{H}_2\text{O})$  for mixed SAMs of  $\text{SC}_{11}\text{E}_n\text{OH}$  ( $n = 2, 4, \text{ and } 6$ ) were almost indistinguishable.

**4. Wettability Was Only a General Predictor of Resistance to Protein Adsorption.** Mixed SAMs of  $\text{SC}_{11}\text{OH}$  adsorbed more

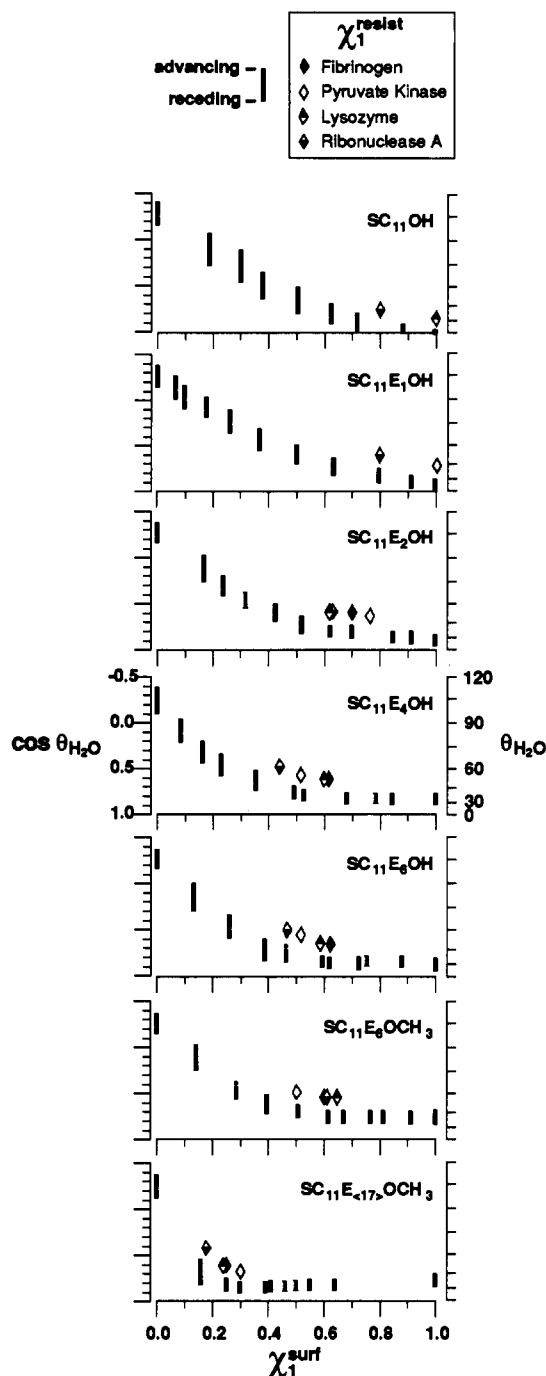


**Figure 4.** Wettability as a function of  $\chi_1$ . The wettability of mixed SAMs of  $\text{SC}_{11}\text{E}_n\text{OR}$ —as measured by  $\cos \theta_a(\text{H}_2\text{O})$  and  $\cos \theta_r(\text{H}_2\text{O})$ , the maximum advancing and minimum receding contact angles of water on the SAMs—increased as a function of  $\chi_1$ , the mole fraction of  $\text{SC}_{11}\text{E}_n\text{OR}$  chains in the SAM. Each symbol in the plot is bounded above by the value of  $\cos \theta_a(\text{H}_2\text{O})$  and below by the value of  $\cos \theta_r(\text{H}_2\text{O})$ . The length of the symbol represents the hysteresis in the contact angle of water,  $|\cos \theta_a(\text{H}_2\text{O}) - \cos \theta_r(\text{H}_2\text{O})|$ . The diamonds indicate the values of  $\chi_1^{\text{resist}}$  for each of the four proteins studied. The horizontal and vertical scales of the plots are uniform throughout the figure.

protein than mixed SAMs of  $\text{SC}_{11}\text{E}_n\text{OH}$  ( $n \geq 1$ ), although pure SAMs of  $\text{SC}_{11}\text{OH}$  were more hydrophilic than pure SAMs of  $\text{SC}_{11}\text{E}_n\text{OH}$  ( $n \geq 1$ ). Methoxy-terminated chains resisted adsorption at lower (more hydrophobic) values of  $\cos \theta_a(\text{H}_2\text{O})$  than hydroxyl-terminated chains.

**Effects of Temperature.** The majority of experiments reported here were carried out using solutions at 25 °C. Proteins are often encountered by materials at other temperatures. We examined the dependence of the adsorption of pyruvate kinase onto mixed SAMs of  $\text{SC}_{11}\text{E}_6\text{OH}$  upon the temperature at which the adsorption

(41) Lyman, D. J.; Muir, W.; Lee, I. J. *Trans. Am. Soc. Artif. Intern. Organs* 1965, 11, 301–306. Nyilas, E.; Morton, W. A.; Lederman, D. M.; Chiu, T. H.; Cumming, R. D. *Trans. Am. Soc. Artif. Intern. Organs* 1975, 21, 55–69. Kaelble, D. H.; Moacanin, J. *Polymer* 1977, 18, 475–482. Coleman, D. L.; Gregonis, D. E.; Andrade, J. D. *J. Biomed. Mater. Res.* 1982, 16, 381–398.

(42) Norde, W. *Adv. Colloid Interface Sci.* 1986, 25, 267–340.

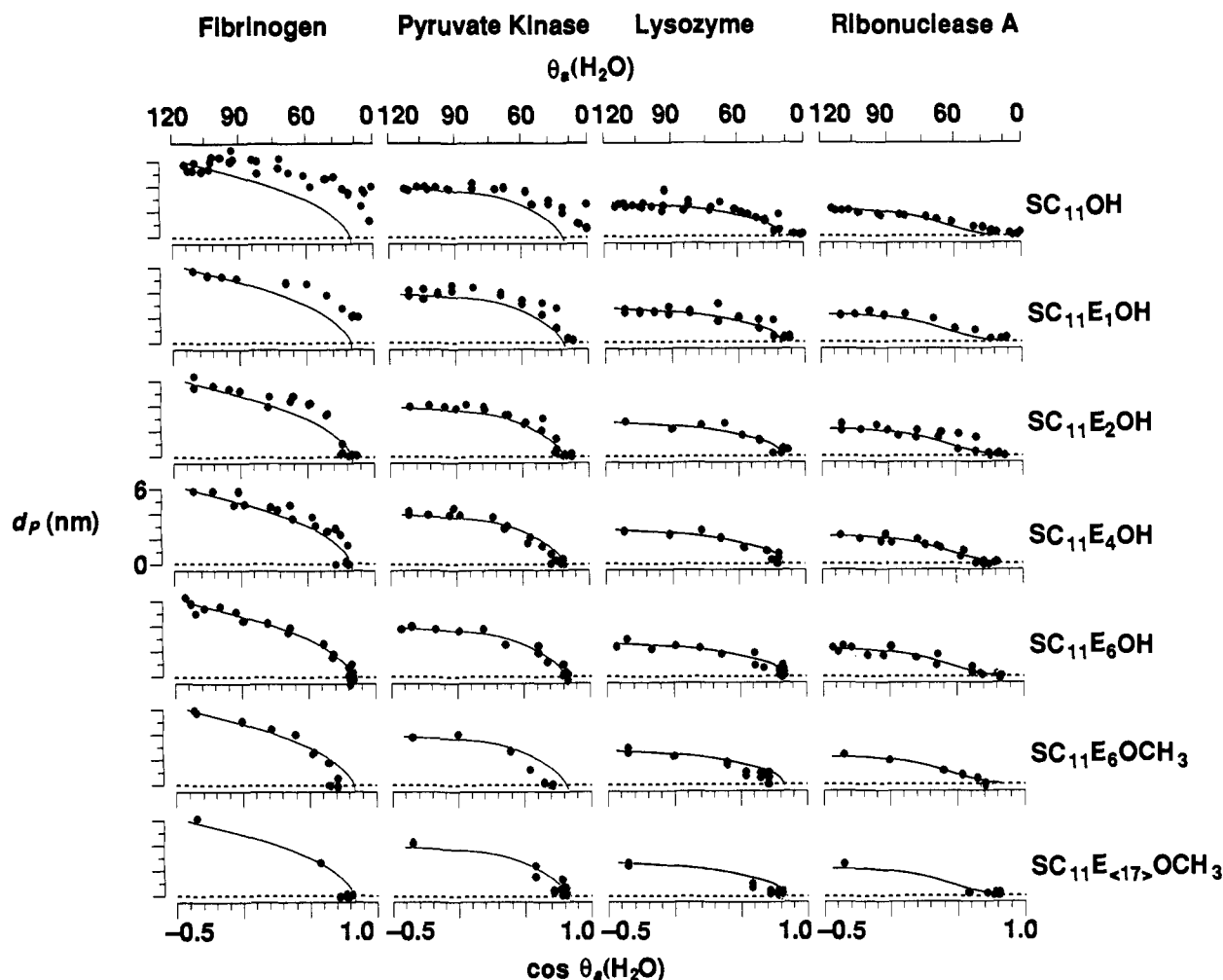


**Figure 5.** Nominal thickness ( $d_p$ ) as a function of wettability. Adsorption of proteins to mixed SAMs of  $SC_{11}E_nOR$  is sensitive to the presence of accessible hydrophobic regions. The nominal thickness  $d_p$  of adsorbed films of fibrinogen, pyruvate kinase, lysozyme, and ribonuclease A on mixed SAMs of  $SC_{11}E_nOR$  is plotted as a function of the wettability—represented by  $\cos \theta_s(H_2O)$ —of the SAM. The vertical and horizontal scales are uniform throughout the figure. The solid curves in each column are the same. They are taken from the data for  $SC_{11}E_6OH$  in that column and are reproduced on each graph to aid comparison among them.

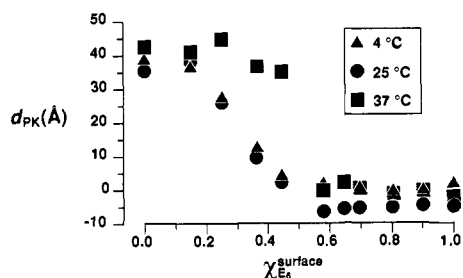


**Figure 6.** Nominal thickness of the film of adsorbed pyruvate kinase,  $d_{PK}$  as a function of the mole fraction of  $SC_{11}E_6OH$  in the SAM. Mixed SAMs of  $SC_{11}E_6OH$  for which  $\chi_1 < \chi_1^{resist}$  adsorbed more pyruvate kinase at 37 °C than at lower temperatures. There was no experimentally significant difference between the adsorption at 4 and 25 °C. The value of  $\chi_1^{resist}$  did not change over the range of temperatures shown.

and rinsing were carried out. Figure 6 shows the value of  $d_p$  as a function of  $\chi_1$  and  $T$ . The adsorption profiles were sensitive to temperature. There was no significant difference between adsorption at 4 and 25 °C. The adsorption at 37 °C differed in that mixed SAMs with  $\chi_1 < \chi_1^{resist}$  appeared to be less resistant to adsorption. The value of  $\chi_1^{resist}$  was independent of temperature.

## Discussion

**Origin of Resistance of EO SAMs to Adsorption of Proteins.** The most striking observation derived from the data presented

in Figure 3 and 5 is the similarity between the shapes of the adsorption curves of the different proteins on each series of mixed SAMs. Lysozyme<sup>43</sup> and ribonuclease<sup>44</sup> are globular proteins with molecular weight approximately 15 000 Da; pyruvate kinase is a noncovalent tetramer of 55 000-Da subunits,<sup>45</sup> and fibrinogen is a structurally complex, flexible molecule of approximately 340 000 Da.<sup>46</sup> The number of EO chains per unit area required to eliminate adsorption was almost the same for each of the four. The similar behavior of different proteins on the same surface suggests that the adsorbance of each mixed SAM is dominated by the interfacial properties of the SAM, not by those of the protein.

We sought to relate a useful parameter of resistance to protein adsorption to some structural property of the SAM. The properties of polymers can frequently be expressed as power laws of the lengths of the polymer chains.<sup>47</sup> We fitted the value of  $\chi_1^{resist}$  to such a power law:  $\chi_1^{resist} = k_1 n^{k_2}$ . The values of  $k_1$  and  $k_2$  were determined by least-squares analysis for each of the four proteins. The average value of  $k_2$  was  $-0.4 \pm 0.05$ ;  $k_1$  ranged from 0.8 to 1.1 (see Figure 7). In Figure 7, we plotted the value of  $\chi_1^{resist}$  as a function of  $n^{-0.4}$  for all four proteins combined and

(43) Imoto, T.; Johnson, L. N.; North, A. C. T.; Phillips, D. C.; Rupley, J. A. *The Enzymes*, 3rd ed.; Academic: New York, 1972; Chapter 21.

(44) Wlodawer, A.; Svensson, L. A.; Sjoelin, L.; Gilliland, G. L. *Biochemistry* **1988**, *27*, 2705–2717.

(45) Muirhead, H. *Biol. Macromol. Assem.* **1987**, *3*, 143–186.

(46) Shafer, J. A.; Higgins, D. C. *Crit. Rev. Clin. Lab. Sci.* **1988**, *26*, 1–41.

(47) De Gennes, P. G. *Scaling Concepts in Polymer Physics*; Cornell University: Ithaca, NY, 1979.

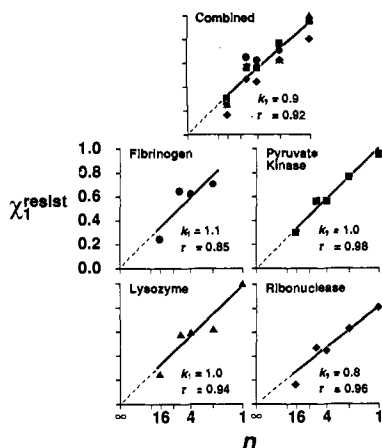


**Figure 7.** Values of  $\chi_1^{\text{resist}}$  plotted as a function of  $n^{-0.4}$ . The resistance of mixed SAMs of **1** to the adsorption of proteins, as measured by  $\chi_1^{\text{resist}}$ , is proportional to  $n^{-0.4}$ , where  $n$  is the number of monomer units per chain. The curve fits for the individual proteins were made by least-squares analysis to a line passing through the origin. The curve fit for the combined data was made by least-squares analysis to a line. The slopes  $k_1$  and correlation coefficients  $r$  of the fits are displayed on each plot. The horizontal and vertical axes are uniform in scale and meaning throughout the figure.

for each protein alone. The solid lines in these plots represent calculated fits to the equation  $\chi_1^{\text{resist}} = k_1 n^{-0.4}$ . The fits were therefore constrained to pass through the origin, in agreement with the requirement that  $\chi_1^{\text{resist}} \rightarrow 0$  as  $n \rightarrow \infty$ . These plots demonstrate that *most of the decrease in  $\chi_1^{\text{resist}}$  (and increase in protein resistance) observed in these systems as  $n$  increases from 1 to 17 is accounted for by the increased length of the EO chains incorporated in the SAMs.*

In a treatment of the conformations of polymers attached to interfaces, de Gennes<sup>48</sup> pointed out that the expected average number of monomer groups per unit area at a distance  $R_F$  from the surface,  $\phi(z = R_F)$ , should be related to the grafting density  $\sigma$  and to the length of the chains  $N$  by the equation  $\phi(z = R_F) \approx \rho N^{2/5}$ . This equation is only rigorously valid in cases where the individual chains are long ( $N > 100$ ) and do not interact with one another ( $\sigma < 1/(N^{6/5})$ ). The experiments reported here were performed with short chains ( $N \leq 17$ ) that were present in greater numbers per unit area than  $1/(N^{6/5})$ . Despite these limitations on the applicability of our data, the agreement between the exponent of  $N$  derived from theory and the exponent observed in these experiments is remarkable.

**Steric Repulsion.** Our observations show that very short EO-containing chains ( $N \geq 1$ ) can effectively resist the adsorption of proteins to hydrophobic substrates. In contrast, a number of workers<sup>49–52</sup> have recently found that very long chains of grafted poly(ethylene oxide) are optimal for making surfaces protein-resistant. This apparent conflict is not as serious as it seems at first. Our results suggest that the principal benefit derived from longer chains is that coverage of the substrate can be achieved with fewer chains. The self-assembly process can prepare films with much greater numbers of EO chains per unit area than most chemical grafting methods. In the limits of low values of  $\chi_1$  ( $0 < \chi_1 < 0.1$ ), our data show that longer chains do indeed reduce protein adsorption (see Figure 3), an observation consistent with those of other workers. Our data lead us to conclude that the principal criterion for protein resistance in these systems is complete coverage of the surface by an EO film of any thickness

(48) De Gennes, P. G. *Macromolecules* **1980**, *13*, 1069–1075.

(49) Desai, N. P.; Hubbell, J. A. *J. Biomed. Mater. Res.* **1991**, *25*, 829–843.

(50) Desai, N. P.; Hubbell, J. A. *Biomaterials* **1991**, *12*, 144–153.

(51) Gombotz, W. R.; Wang, G.; Horbett, T. A.; Hoffman, A. S. *J. Biomed. Mater. Res.* **1991**, *25*, 1547–1562.

(52) Bergström, K.; Homberg, K.; Safranji, A.; Hoffman, A. S.; Edgell, M. J.; Kozłowski, A.; Hovanes, B. A.; Harris, J. M. *J. Biomed. Mater. Res.* **1992**, *26*, 779–790.

and that longer chains simply cover the surface more effectively than shorter chains. Recent reports of dramatically reduced protein adsorption to hydrophobic surfaces that are grafted-polymerized with tetra(ethylene glycol) derivatives confirm this interpretation.<sup>53</sup>

Then, are our data compatible with the hypothesis that steric repulsion (as applied to the stabilization of colloids by polymers) is important in resisting protein adsorption? Jeon and Andrade<sup>20</sup> made three predictions based upon their calculations: (i) that the optimal density of PEO chains for resistance to protein adsorption decreases as the size of the protein increases; (ii) that chains of PEO packed near the density of crystalline PEO should be less resistant to protein adsorption than less closely packed chains; and (iii) that at the optimum value of  $\chi_1$ , longer chains are more resistant to adsorption. The limited data in this study do not provide a substantial test of these predictions. We observed no optimum value of  $\chi_1$ , only a threshold value. The most closely packed chains of EO we observed ( $\chi_1 = 1$ ) were entirely resistant to adsorption. The packing of these chains is, however, still sufficient to provide substantial volume for water. We did observe that longer chains had lower values of  $\chi_1^{\text{resist}}$  and lower values of  $d_P$  at constant values of  $\chi_1$ .

**Adsorption in Situ.** The technique that we employed to measure  $d_P$  in these studies involved removing the samples from solution and rinsing them. An observation of  $d_P = 0$  means that no protein was able to adsorb strongly enough to resist the shear of rinsing. Is it possible that protein adsorbs weakly to mixed SAMs of EO *in situ*? Our observations suggest, but do not prove, that such weak adsorption occurs.

When a SAM of **1** that has not been exposed to protein is rinsed with water, the water runs off the sample leaving a dry surface (the value of  $\theta_r(\text{H}_2\text{O})$  is greater than  $0^\circ$ ). This same phenomenon is observed when rinsing protein solutions from mixed SAMs of **1** for which  $d_P = 0$ . Water does not run off mixed SAMs of **1** for which  $d_P > 0$ ; instead, it forms a thin film ( $\theta_r(\text{H}_2\text{O}) = 0^\circ$ ). The protein solutions do not run off of any SAM, even those for which  $d_P = 0$ . One rationalization of this observation would be the presence of an adsorbed film of protein that persists until the first rinse removes it. Another would be that the dissolved proteins lower  $\gamma_{lv}$  enough to make  $\theta_r(\text{H}_2\text{O}) = 0^\circ$ . We can not presently distinguish between these alternatives.<sup>54</sup>

**Temperature Effects.** There are at least two reasons for thinking that the resistance of mixed SAMs of **1** toward protein adsorption might decrease with increasing temperature. First, the “hydrophobic effect” is expected to increase with increasing temperature.<sup>55</sup> Second, EO chains are known to have lower solubility limits at elevated temperatures,<sup>56</sup> an effect that is usually ascribed to a negative entropy of solvation of EO groups by water. Such an effect would render EO chains at an interface less hydrophilic

(53) Lopez, G. P.; Ratner, B. D.; Tidwell, C. D.; Haycox, C. L.; Rapoza, R. J.; Horbett, T. A. *J. Biomed. Mater. Res.* **1992**, *26*, 415–439.

(54) Proteins are surfactants, and it has been known for half a century (Neurath, H.; Bull, H. B. *Chem. Rev.* **1938**, *23*, 391–435) that the air–solution surface tensions of protein solutions are time-dependent and significantly lower than the surface tension of the air–water interface. The receding contact angle of water on EO surfaces is approximately  $25^\circ$  ( $\cos \theta_r(\text{H}_2\text{O}) = 0.9$ ). By the application of Young’s Equation (Young, T. *Philos. Trans. R. Soc. London* **1805**, *95*, 65–87),  $\cos \theta = (\gamma_{lv} - \gamma_{sl})/\gamma_{sv}$ , two liquids with different values of  $\gamma_{lv}$  and equal values of  $\gamma_{sl}$  will have contact angles that are related by  $\cos \theta_1 \gamma_{lv}^{(1)} = \cos \theta_2 \gamma_{lv}^{(2)}$ , where the numerical sub- and superscripts  $i$  refer to liquid  $i$ . Setting  $\theta_1 = 25^\circ$ ,  $\gamma_{lv}^{(1)} = 72$  dyn/cm (the air–water surface tension at  $25^\circ\text{C}$ ), and  $\theta_2 = 0^\circ$ , we estimate that solutions with air–solution surface tensions less than approximately 65 dyn/cm will have values of  $\theta_r(\text{H}_2\text{O}) = 0^\circ$ . The value of  $\gamma_{lv}$  for 0.1% solutions of egg albumin (the same concentration at which our experiments were performed) drops to less than 65 dyn/cm in a matter of seconds (Hauser, E. A.; Swearingen, L. E. *J. Phys. Chem.* **1941**, *45*, 644–659). Precise determination of  $\gamma_{lv}$  for solutions containing proteins is experimentally difficult. In our experiments, the surface area of the protein solution changes rapidly as the sample is removed from the adsorption vial. This additional complication makes the determination of a relevant value of  $\gamma_{lv}$  very difficult. Some further evidence for a lowered value of  $\gamma_{lv}$  is available through our observation that the protein solutions used in this study often form foams that remain stable from minutes to hours.

(55) Sharp, K. A. *Curr. Opin. Struct. Biol.* **1991**, *1*, 171–174. Privalov, P. L.; Gill, S. J. *Pure Appl. Chem.* **1989**, *61*, 1097–1104.

and possibly less resistant to protein adsorption at higher temperatures than at lower ones.

We investigated the effect of temperature upon the adsorption of pyruvate kinase to mixed SAMs of  $SC_{11}E_6OH$ . The results are shown in Figure 6. There is no significant difference between the curves for  $T = 4\text{ }^{\circ}C$  and  $T = 25\text{ }^{\circ}C$ . We do not know why the SAMs at  $25\text{ }^{\circ}C$  gave values of  $d_p < 0$ , but note that their wettabilities after immersion in the protein solution were the same as those of SAMs for which  $d_p = 0$ . There was a significant difference between  $T = 25\text{ }^{\circ}C$  and  $T = 37\text{ }^{\circ}C$ , in which mixed SAMs for which  $\chi_1 < \chi_1^{\text{resist}}$  adsorbed more protein at the higher temperature. The value of  $\chi_1^{\text{resist}}$  remained constant, however.

## Experimental Section

**Materials.** Test-grade, 100-mm, singly polished silicon wafers (Silicon Sense), chromium (99.99%, Aldrich), and gold (99.999% as machined pellets, Materials Research Corp.) were used as received.

Fibrinogen (fraction I from human plasma, Sigma), pyruvate kinase (EC 2.7.1.40, type PK-3 from rabbit muscle, Biozyme), lysozyme (EC 3.2.1.17, grade III from chicken egg white, Sigma), and ribonuclease A (EC 3.1.27.5, type III-A from bovine pancreas) were used as received. Buffer solutions were prepared from disodium hydrogen phosphate (0.010 M) and titrated to pH 7.5 with phosphoric acid.

Absolute ethanol (US Industrials Co.) was used as received. Deionized water was distilled from glass in a Corning Ag-1b still.

**Preparation of Gold Substrates.** Gold substrates were prepared by evaporating first Cr (10 nm) and then Au (200 nm) onto silicon wafers in a two-gun electron-beam evaporator. The evaporations were performed at a pressure of  $2 \times 10^{-7}$  Torr and a rate of 0.5 nm/s for both metals. The Cr was evaporated as an adhesion layer between the oxidized Si surface and the Au. The Au substrates were stored in poly(propylene) wafer carriers and immersed in thiol solutions within an hour after they were removed from the vacuum chamber.

**Solutions of Alkanethiols.** Volumetric flasks were rinsed thoroughly with water, then treated with freshly prepared piranha solution (a 7:3 v/v mixture of concentrated  $H_2SO_4$  and 30% aqueous  $H_2O_2$ ) for 30 min at  $90\text{ }^{\circ}C$ , rinsed thoroughly with distilled, deionized water, and dried in an oven. Disposable glass scintillation vials (20 mL) were used for the adsorption solutions without cleaning. *Caution: Piranha solution reacts violently with many organic materials and should be handled with extreme care.*

Stock solutions (2.5 mM) of alkanethiols in absolute ethanol were prepared fresh and used to make adsorption solutions. The adsorption solutions were prepared by mixing aliquots of two stock solutions (total volume = 2 mL) and diluting the solution to 20 mL with absolute ethanol.

**Preparation of SAMs.** Gold substrates were cut into pieces ( $\approx 3$  cm  $\times$  1 cm) with a diamond-tipped stylus, dusted free of debris with a stream of nitrogen, and immersed in the adsorption solutions for at least 8 h. For each experiment, two SAMs were prepared simultaneously in each adsorption solution. One SAM was used to obtain XPS, ellipsometry, and contact angle data; the other was used for protein adsorption studies.

**X-ray Photoelectron Spectroscopy (XPS).** XPS spectra were obtained on an SSX-100 spectrometer (Surface Science Instruments) using an Al  $K\alpha$  source, a quartz monochromator, a concentric hemispherical analyzer in transmission mode, and a multichannel detector. The spectra were accumulated at a take-off angle of  $35^{\circ}$  relative to the surface and a pressure of  $(2-8) \times 10^{-9}$  Torr. Spectra were fitted using software from Surface Science Instruments. O(1s) peaks were modeled as 80% Gaussian/20% Lorentzian functions; Au( $4f_{7/2}$ ) and Au( $4f_{5/2}$ ) peaks were modeled as 70% Gaussian/30% Lorentzian functions. The choice of functions was empirical; these values gave the best fits to the experimental data. The areas under the modeled peaks were used to calculate values of  $\chi_1$ .

**Ellipsometry.** Ellipsometric measurements were made with a Rudolf Research Type 43603-200E manual thin-film ellipsometer operating at 632.8 nm (He-Ne laser) and an angle of incidence of  $70^{\circ}$ . The PCSA (polarizer-compensator-sample-analyzer) configuration was used with the compensator set to  $-45^{\circ}$ . Three separate values of  $d_p$  were determined on each SAM by obtaining the ellipsometric constants of the SAM immediately before it was immersed in the protein solution and after it was rinsed following the immersion (see below). The values of  $d_p$  were

calculated with a planar, three-layer (ambient-protein-SAM) isotropic model<sup>36</sup> with assumed refractive indices of 1.00 and 1.45 for the ambient and the protein, respectively. The values of  $d_p$  reported here are the averages of the three values on each SAM.

Determination of the thicknesses of mixed SAMs of **1g** and **2** was carried out using the same model (this time, ambient-SAM-substrate with refractive indices of 1.00 and 1.45 for the ambient and the SAM, respectively); however, the ellipsometric constants were measured before and after immersion of the gold substrate in the thiol adsorption solution.

**Contact Angles.** Contact angles were determined at ambient laboratory temperatures ( $20-25\text{ }^{\circ}C$ ) with a Ramé-Hart Model 100 contact-angle goniometer. Water was dispersed from a Matrix Technologies Microelectropipette. We measured the maximum advancing and minimum receding contact angles.<sup>33</sup> The reported values are the average of three measurements taken at different locations on the SAM.

**Protein Adsorption Experiments.** Protein solutions were prepared by dissolving the protein sample (120 mg) in cold ( $5\text{ }^{\circ}C$ ) 10 mM phosphate buffer (pH 7.5, 120 mL) and allowing the solutions to warm to ambient temperatures. This quantity of solution was enough to fill six 20-mL scintillation vials with a total capacity of 12 SAMs. Samples of fibrinogen contained about 50% protein by weight with the remaining weight consisting of sodium citrate and sodium chloride. Samples of lysozyme contained approximately 85% protein by weight with the remaining weight consisting of sodium acetate and sodium chloride. As a result, the ionic strengths of the solutions formed from these protein samples were higher than the ionic strengths of the other protein solutions.

Individual SAMs were removed one at a time from thiol adsorption solutions, rinsed with ethanol, dried with nitrogen, and placed on the ellipsometer. The ellipsometric constants of the SAM were measured, and the SAM was then immersed in one of the protein solutions. The same process was repeated for as many as 11 more SAMs. After each SAM had been immersed in the protein solution for  $120 \pm 5$  min, it was removed from the protein solution and rinsed with distilled, deionized water. The rinsing procedure consisted of six 1.5-mL aliquots of water applied from a standard disposable Pasteur pipette equipped with a 2-mL rubber bulb. Each SAM was then dried with a stream of nitrogen in order to remove any remaining water before it could evaporate, and the ellipsometric constants of the SAM were measured again.

The technique described above was used to measure  $d_p$  at 25 and 37  $^{\circ}C$ . Before the adsorption experiment was begun, the protein solutions and distilled water for the rinses were equilibrated thermally with a thermostatted water bath at the appropriate temperature. To study adsorption at  $4\text{ }^{\circ}C$  the SAMs were first prepared and analyzed by ellipsometry at  $25\text{ }^{\circ}C$ . The SAMs were stored in poly(propylene) wafer carriers until all had been analyzed—about 1 h for the complete set—and were then taken into a  $4\text{ }^{\circ}C$  cold room. After 30 min, the SAMs were immersed in protein solutions that had been kept in the cold room overnight. After 2 h, the SAMs were removed from the solutions and rinsed with cold ( $4\text{ }^{\circ}C$ ), distilled water. The samples were dried with a stream of  $CHClF_2$  (Chemtronics, Ultrajet ES1270), removed from the cold room all at the same time, stored in the wafer carriers, and analyzed by ellipsometry as soon as possible.

**Acknowledgment.** The authors would like to thank Hans Biebuyck for insightful conversations and Paul Dimilla and Gabriel Lopez for critical readings of the manuscript. Union Carbide Corporation graciously supplied poly(ethylene oxide) of several molecular weights. This research was supported by the National Science Foundation (NSF) under the Engineering Research Center Initiative by a grant to the Massachusetts Institute of Technology Biotechnology Process Engineering Center (cooperative agreement CDR-88-03014), by the Office of Naval Research, and by the Defense Advanced Research Projects Agency (DARPA). The X-ray photoelectron spectrometer was provided by DARPA through the University Research Initiative and is housed at the Harvard University Materials Research Laboratory, an NSF-funded facility. The NMR spectrometer was provided to the Chemical Laboratories of Harvard University through a grant from the NSF (CHE-8410774). K.L.P. was an NSF predoctoral fellow from 1986 to 1989.

**Supplementary Material Available:** Available: Detailed analysis of the methods used for calculating  $d_p$  and  $\chi_1$  and synthetic procedures, spectral data, and analyses of compounds **1b**, **1c**, **1f**, and **1g** (19 pages). Ordering information is given on any current masthead page.

(56) Kjellander, R.; Florin, E. *J. Chem. Soc., Faraday Trans. 1* **1981**, *77*, 2053-2077. Florin, E.; Kjellander, R.; Eriksson, J. C. *J. Chem. Soc., Faraday Trans. 1* **1984**, *80*, 2889-2910. Claesson, P. M.; Kjellander, R.; Stenius, P.; Christenson, H. K. *J. Chem. Soc., Faraday Trans. 1* **1986**, *82*, 2735-2746.